J. del Olmo, F. Garramiola, J. Poza, T. Nieva, G. Almandoz and L. Aldasoro, "DC-link sensor Fault Detection and isolation for railway traction electric drives," 2017 IEEE Workshop on Electrical Machines Design, Control and Diagnosis (WEMDCD), 2017, pp. 244-249.

DOI: https://doi.org/10.1109/WEMDCD.2017.7947754

DC-Link Sensor Fault Detection and Isolation for Railway Traction Drives

Jon del Olmo, Fernando Garramiola, Javier Poza, Txomin Nieva, Leire Aldasoro, Gaizka Almandoz

***Abstract*—This article presents the design and the implementation of a fault detection and isolation strategy for sensors in variable speed drives. Electric drives use several current and voltage sensors for control and protection. The principal objective of the strategy is to detect faults in DC-Link sensors, since the conclusion of a preliminary study showed that in some applications many functionalities depend on it. Although it was mainly designed for DC-Link sensors, thanks to the FDI structure presented here, the algorithm is able to detect faults in other sensors. The strategy is based on state observers and has been validated through real time simulations in a Hardware-in-the-Loop platform. The principal components of the platform are an OPAL-RT real time simulator and a commercial traction control unit.**

***Index Terms*—DC-Link Sensor, Fault Detection, State Observer, Variable Speed Drive, Traction Application**

I. Introduction

In the field of electric drives, Fault Detection and Isolation (FDI) techniques have attracted significant interest over the last decades. With the aim to improve reliability, availability and maintainability, different types of FDI strategies for sensors have been proposed. Most of the work has been developed in the field of current and speed sensor fault detection. Several authors have explored model-based techniques such as state observers [1]–[3] and parity equations [4]-[5] for current sensor fault detection. Moreover, many state observers were designed for sensorless control and speed sensor diagnostics [6]–[9], from electric vehicles to railway traction. Signal based techniques are another alternative for sensor FDI. In [10] an approach to detect current sensor faults in PMSG drives for wind energy conversion is presented. The algorithm only uses current measurements to identify disconnections, as opposed to the conventional model-based solutions. In [11]–[13] current sensor faults are identified analysing current measurements in the dq rotating synchronous reference frame.

Apart from current and speed sensor faults, Direct Current (DC) bus voltage sensor FDI has also been studied. In [14] and [15] a FDI strategy based on state observers is developed for DC-Link sensor faults in a single-phase rectifier for railway traction. The model includes the input filter, the rectifier and the DC-Link voltage to calculate an estimation and reconfigure the system if a fault is detected. A completely different approach is the one presented in [16], where the comparation between the input power and the mechanical output power is the residual calculated for FDI. These methods were specifically designed for DC-Link sensor faults. There are other algorithms that include indirect strategies for DC bus voltage sensor fault detection. [17] and [2] present the development of a Kalman Filter and an adaptive observer respectively. Using the model of the motor and the inverter, they estimate stator currents and mechanical speed. Indirectly, analysing the flags that the FDI strategy activates, they are able to isolate DC bus sensor malfunctions.

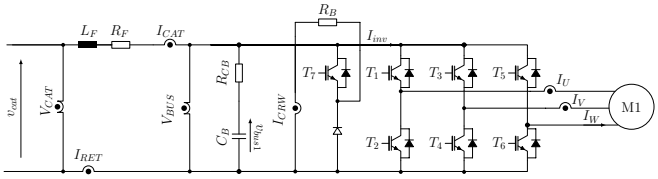

Fig. 1. Electric drive

Among all the sensors installed in electric drives, current and speed sensor faults are the ones that attracted more attention. Even though it is not so obvious, DC-Link sensor faults can equally lead to an emergency stop, for example in railway traction applications. In this kind of electric drives, DC-Link voltage measurements are essential to control regenerative braking, detect pantograph detachments and protect the system against over-voltages. Apart from the aforementioned publications, few authors have addressed this problem directly. Therefore, the objective of our study was the development and validation of a DC bus voltage sensor FDI strategy. A state observer-based algorithm that takes the model of the input LC filter as a reference was designed. The strategy is based on a bank of observers that estimates the DC bus voltage and catenary current.

II. System description and modelling

The diagnostic scheme presented here was designed for a three-phase electric drive supplied by a DC voltage source (see figure 1). For the design of the FDI strategy only the input filter, the DC bus and the braking chopper are considered. Stator phase current sensors and bus voltage sensors are used for control and protection purposes. Catenary voltage and current and crowbar current sensors are used exclusively for protection purposes in railway traction applications.

The model of the input circuit is described by equations (1) and (2):

$$\frac{d\boldsymbol{x}}{dt} = \begin{bmatrix} -\frac{R_F+R_{CB}}{L_F} & -\frac{1}{L_F} \\ \frac{1}{C_B} & 0 \end{bmatrix} \boldsymbol{x} + \begin{bmatrix} \frac{1}{L_F} & \frac{R_{CB}}{L_F} & \frac{R_{CB}}{L_F} \\ 0 & -\frac{1}{C_B} & -\frac{1}{C_B} \end{bmatrix} \boldsymbol{u} \quad (1)$$

This work has been partially supported by the programs: Universidad Empresa (UE-2014-09) and Formación de Investigadores del Departamento de Educación, Universidades e Investigación from the Basque Government.

Jon del Olmo, Fernando Garramiola and Javier Poza are with Mondragon University, Faculty of Engineering, 20500 Mondragon, Spain. (e-mail: jdelolmo,jpoza,fgarramiola,galmandoz@mondragon.edu)

Txomin Nieva and Leire Aldasoro are with CAF Power and Automation, Poligono Katategi, 20271 Irura, Spain. (e-mail: {tnieva,laldasoro}@cafpower.com)

$$\boldsymbol{y} = \begin{bmatrix} 1 & 0 \\ R_{CB} & 1 \end{bmatrix} \boldsymbol{x} + \begin{bmatrix} 0 & 0 & 0 \\ 0 & -R_{CB} & -R_{CB} \end{bmatrix} \boldsymbol{u} \quad (2)$$

where $\boldsymbol{x}^T = \begin{bmatrix} i_{cat} & v_{bus1} \end{bmatrix}$, $\boldsymbol{u}^T = \begin{bmatrix} v_{cat} & i_{inv} & i_{crw} \end{bmatrix}$ and $\boldsymbol{y}^T = \begin{bmatrix} i_{cat} & v_{bus} \end{bmatrix}$.

The current of the DC side of the inverter (i_{inv}) is estimated using the phase currents and the IGBT state signals as follows:

$$i_{inv} = i_u \cdot S_1 + i_v \cdot S_3 + i_w \cdot S_5 \quad (3)$$

where S_1, S_3 and S_5 are the switching states of the upper side semiconductors and i_w is the current of the third phase.

III. Sensor fault detection and isolation strategy

A. Fault detection structure

As it is shown in figure 2, the FDI process has three steps: feature generation, fault detection and fault isolation. In the first step features that could indicate the existence of a fault are generated. In this case, a bank of two observers estimates the state variables of the system. Both observers are based on the model of the input filter and estimate the bus voltage and the input current. To estimate both state variables, the same observer structure (figure 3) is executed twice using only the measurement of the catenary current (i_{cat}) or the measurement of the DC bus voltage (v_{bus}) and their respective configuration.

Once the estimations are generated the fault detection is executed. Firstly, each estimation is compared to a measurement to obtain the residuals (4)-(7). Subscripts indicate the variable and the superscripts the observer used for the estimation.

$$r_{cat}^{cat} = i_{cat} - \hat{i}_{cat}^{cat} \quad (4)$$

$$r_{bus}^{cat} = v_{bus} - \hat{v}_{bus}^{cat} \quad (5)$$

$$r_{cat}^{bus} = i_{cat} - \hat{i}_{cat}^{bus} \quad (6)$$

$$r_{bus}^{bus} = v_{bus} - \hat{v}_{bus}^{bus} \quad (7)$$

After the residuals are calculated, the fault detection algorithm decides which fault flags (f) to activate. In real applications, residuals can not be directly used as fault indicators, since they can be corrupted by noise or affected by operation point changes. Therefore, thresholds should be selected carefully [14] [18]. To avoid false alarms, flags are activated only when

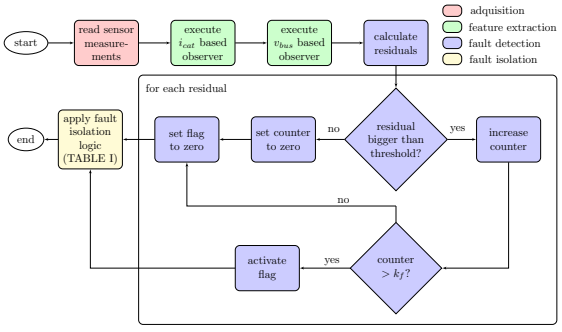

Fig. 2. FDI process flow chart

TABLE I
Fault isolation logic

Faulty sensor	v_{bus}	i_{cat}	v_{cat}	i_u, i_v, i_{crw}
f_{cat}^{cat}	0	1	1	0
f_{bus}^{cat}	1	1	1	0
f_{cat}^{bus}	1	1	1	1
f_{bus}^{bus}	1	0	1	0

its corresponding residual exceeds a limit for at least the time specified by T_{fault}. This parameter is defined as:

$$T_{fault} = k_f \cdot h \quad (8)$$

where k_f is the number of samples and h is the sampling period.

The value of k_f will establish the sensitivity of the algorithm. If k_f is too large, the false alarm rate will be low, because the FDI strategy will not be disturbed by noise or operation point changes. However, the sensitivity will get worse and it may not detect some faults. If k_f is to small, false alarms will increase but the system will be very sensitive to any change in the residuals.

Finally, the identification of faults is performed. Each type of fault makes the group of residuals and flags react in a different way. Following an isolation logic (see table I) the specific fault can be identified. This logic was deduced during the design stage of the algorithm and corroborated by the experimental results (see section IV).

B. Observer design

For the estimation of i_{cat} and v_{bus} two Luenberger state observers [19], [20] were used. These observers, previously presented in figure 3, are described by equations (9) and (10).

$$\dot{\hat{x}}(t) = A\hat{x}(t) + Bu(t) + L(y(t) - \hat{y}(t)) \quad (9)$$

$$\hat{y}(t) = C\hat{x}(t) + Du(t) \quad (10)$$

Thanks to the feedback matrix L one can change the dynamics of the system to minimise the estimation error. Parameter uncertainties and modelling errors make the use of an open loop configuration troublesome, so the measurements are fedback using matrix L. The dynamics in closed loop are defined by matrix $A - LC$. In this case, taking into account that only one measurement is used per observer in the feedback, the feedback matrices are:

$$L_{cat} = \begin{bmatrix} l(1,cat) & l(2,cat) \end{bmatrix}^T \; L_{bus} = \begin{bmatrix} l(1,bus) & l(2,bus) \end{bmatrix}^T$$

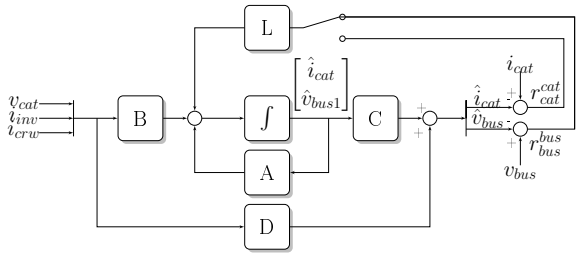

Fig. 3. Observer based on the measurement of i_{cat}

The closed loop poles are obtained solving equation 11. It is worth mentioning that the output matrix C is modified to only consider the elements related to the measurement used in the feedback.

$$det(sI - A + L_{cat}C) = \begin{bmatrix} s - a_{11} + l_1^{cat} & -a_{12} \\ -a_{21} + l_2^{cat} & s - a_{22} \end{bmatrix} = 0 \quad (11)$$

where

$$a_{11} = -\frac{R_F + R_{CB}}{L_F}, a_{12} = -\frac{1}{L_F}, a_{21} = -\frac{1}{C_B}, a_{22} = 0$$

As a result, closed loop poles are obtained:

$$p_{1,2}^{cl} = \frac{a_{11} + a_{22} - l_1^{cat}}{2} \pm \frac{1}{2}\sqrt{(l_1^{cat} - a_{11} - a_{22})^2 - 4(a_{22}(a_{11} - l_1) + a_{a12}(l_2 - a_{21}))}$$

The values for the matrix components l_1 and l_2 are calculated once the poles in closed loop are chosen. These poles are fixed using parameters n and m that relate open loop poles with closed loop poles as follows:

$$\begin{cases} n \cdot \Re\{p_{1,2}^{ol}\} = \Re\{p_{1,2}^{cl}\} \\ m \cdot \Im\{p_{1,2}^{ol}\} = \Im\{p_{1,2}^{cl}\} \end{cases} \quad (12)$$

The closed loop values should stablish a faster system dynamic than the open loop poles. In this regard, it must be pointed out that a balance has to be found between the dynamic of the observer and its sensitivity to noise. If the observer is too fast it will track measurement noise rather than the variable [19]. Moreover, taking into account that this is a FDI application, observer dynamics will also affect the way residuals respond to faults. The DC-bus voltage-based observer is designed following the same steps, taking v_{bus} as output variable.

C. Observer stability and robustness

One of the weaknesses of model-based detection methods is parameter uncertainty. State observers are based on nominal models and it is supposed that parameters such as filter capacity and inductance do not change. Nevertheless, faults or wear could modify their values deteriorating the performance of the observers. Some authors have designed adaptive observers to solve this problem. In any case, it is worth mentioning that the selection of the input filter as the system for state estimation partly helps avoid this problem. Filter inductance and capacitor parameters tend to change less with different operation points compared to motor parameters. Moreover, it is easier to foresee parameter variations in these components than in induction motors, where many variables (current, saturation, temperature, ...) have to be analysed. This is one of the reasons why this approach was selected over the solutions analysed in section I, where the model of the motor is the main tool to detect faults in sensors.

In order to check the stability and robustness of the observers, the same closed loop configuration has been tested for different C_B and L_F values. These parameters have been

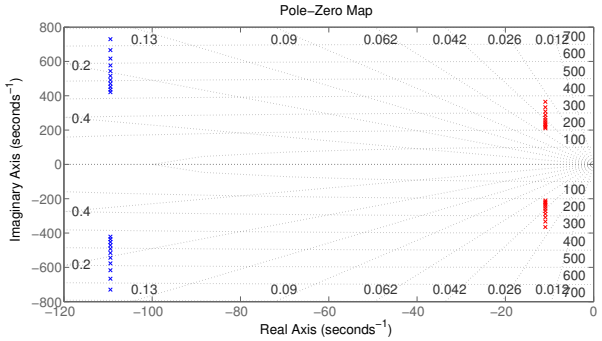

Fig. 4. Open loop and closed loop poles with variable C_B

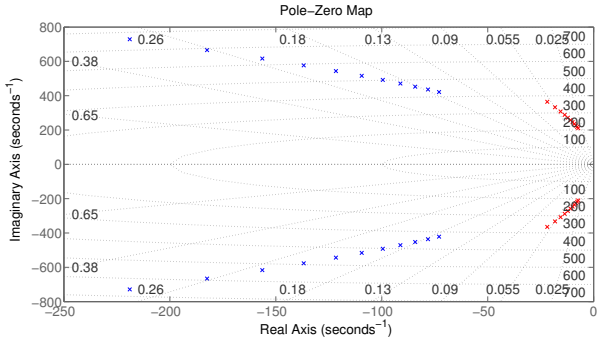

Fig. 5. Open loop and closed loop poles with variable L_F

modified from 50% to 150% of their nominal value. Figures 4 and 5 show the poles in closed and open loop for different parameter values. As it can be seen both observers are stable. For Metallized Polypropylene Film (MPPF) capacitors, a 2% loss of capacitance is usually considered as the threshold to replace them. Therefore it will be unusual to find capacitors with a capacitance variation greater than that.

IV. Experimental results

The proposed algorithm has been validated in a Hardware-in-the-Loop (HIL) platform consisting of an OPAL-RT real time simulator and a Traction Control Unit (TCU) developed by CAF Power & Automation. The model of the traction drive is executed in the OPAL-RT real time simulator, while the control and the proposed FDI algorithm run in the TCU.

The model of the electric drive has been implemented and simulated in the real time simulator using Matlab/Simulink. The model also includes a fault injection block for sensors. This block allows testing the response of the system to faults such as offset, gain and disconnection. The parameters of the system are: $v_{cat} = 750V$, $L_F = 3mH$, $R_F = 64m\Omega$ and $R_{CB} = 1.68m\Omega$. It is considered that only one sensor can fail at a time.

The threshold values selected for the residuals in the experimental tests are 10 A for current residuals (r_{cat}^{cat}, r_{cat}^{bus}) and 20 V for voltage residuals (r_{bus}^{cat}, r_{bus}^{bus}). These are the minimum values to avoid false alarms in fault-free operation taking into account the overall working conditions. These conclusions were drawn from several HIL experimental tests done to characterize the effects of the faults. In a practical implementation these threshold values could be increased in

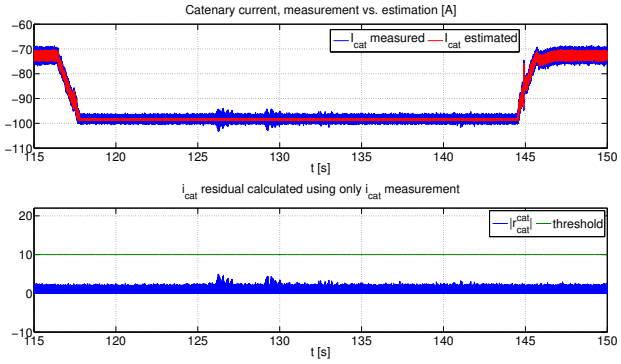

Fig. 6. Measurement and estimation of i_{cat} with i_{cat}-based observer

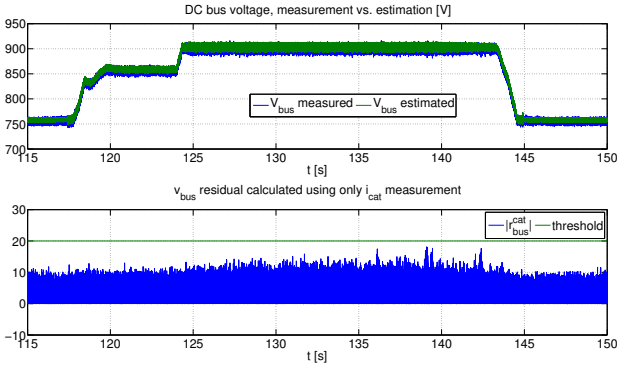

Fig. 7. Measurement and estimation of v_{bus} with i_{cat}-based observer

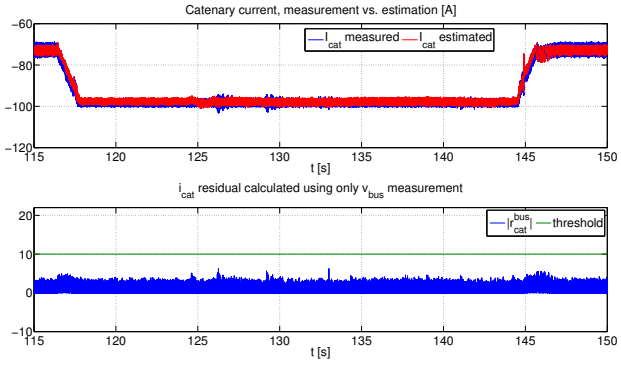

Fig. 8. Measurement and estimation of i_{cat} with v_{bus}-based observer

order to allow higher error levels in the sensors before an error flag is activated.

A. Fault free observer response

Before analysing the FDI system response to faults, its behaviour under healthy conditions was assessed. To this end, each residual was monitored to see the performance of the observer during transient and steady states. The aim of these simulations was to verify that the residuals are below the thresholds when there is no fault. Figures 6-9 show the estimations during transients in the catenary current and DC-Link voltage. Residuals are also presented. Threshold values for each residual were selected taking into account experimental simulations and the required sensitivity for the algorithm.

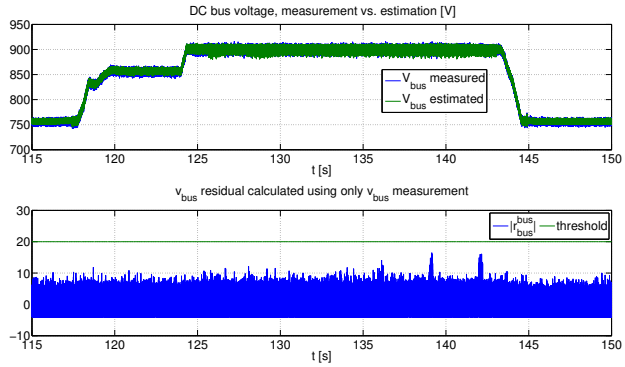

Fig. 9. Measurement and estimation of v_{bus} with v_{bus}-based observer

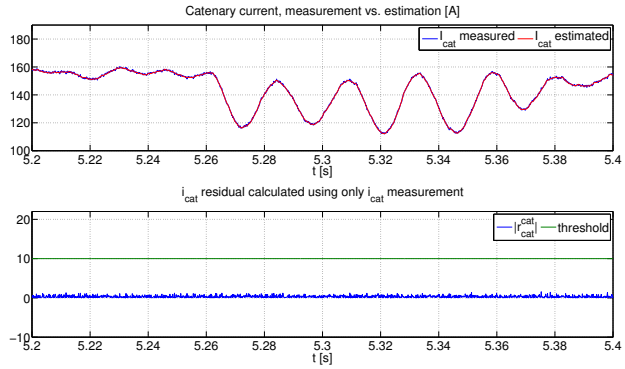

Fig. 10. Measurement and estimation of i_{cat} with i_{cat}-based observer. v_{bus} sensor fault

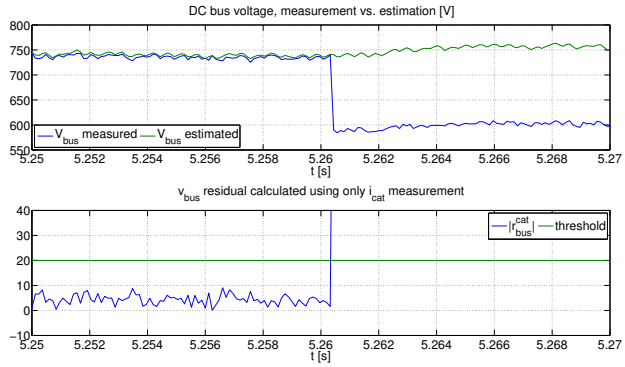

Fig. 11. Measurement and estimation of v_{bus} with i_{cat}-based observer. v_{bus} sensor fault

B. Observer response to DC-Link sensor faults

In order to see the response of the FDI strategy to DC bus voltage sensor faults, gain (higher and lower measurement) and disconnection faults were simulated. The response of the bank of observers in all three cases is the same. In figures 10 and 11 can be seen that the residual r_{cat}^{cat} does not change as a consequence of a 20% gain reduction fault, while r_{bus}^{cat} exceeds the threshold. The residuals generated with the v_{bus}-based observer estimations are also higher than the limits. It was concluded from HIL simulations that the strategy is also sensitive to incipient DC-Link sensor faults.

C. Observer response to catenary current sensor faults

Even thought the main objective was not to detect faults in i_{cat} sensors, thanks to the state-observer structure there will

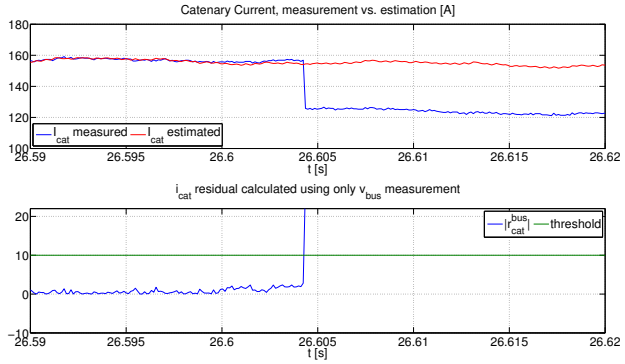

Fig. 12. Measurement and estimation of i_{cat} with v_{bus}-based observer. i_{cat} sensor fault

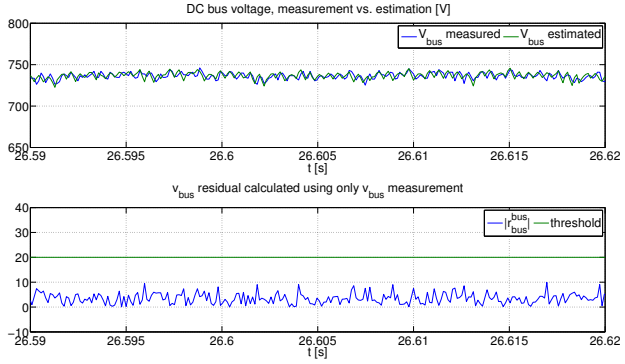

Fig. 13. Measurement and estimation of v_{bus} with v_{bus}-based observer. i_{cat} sensor fault

always be a healthy i_{cat} estimation available. Figures 12 and 13 present the response of the observers to a 20% reduction in the sensor gain. It can be seen that the r^{bus}_{bus} residual is below the limits, therefore it can be distinguished from the previous fault.

D. Observer response to faults in other sensors

The model used for the estimation of v_{bus} and i_{cat} has as inputs i_{crw}, v_{cat} and i_{inv}. i_{inv} is estimated using phase current measurements. In order to identify effectively v_{bus} and i_{cat} sensor faults, the faults in the rest of the sensors should activate another combination of flags. As an example, the effect of a 20% gain reduction in phase u current sensor is shown in figures 14-17. The rest of the faults (in v_{cat} and i_{crw} sensors) were also simulated to define the fault isolation logic, but more detailed results are not shown due to lack of space.

E. Fault isolation logic

As it has been said before, faults in v_{bus} and i_{cat} activate a unique flag combination. This is also the case of the catenary voltage sensor faults. However, there is no direct way to distinguish among phase current sensor faults and braking chopper sensor faults. Both events activate the same flag combination and it is not possible to isolate the fault. This fact does not cause any problem in a real railway application because there are operation modes where the braking chopper is not activated for a long time. In these operation modes, phase current sensor faults can be detected directly. If these phase current sensors are healthy but the flag is activated, a chopper current sensor fault is diagnosed.

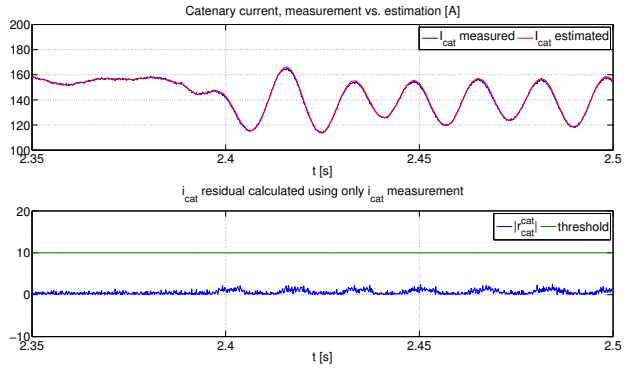

Fig. 14. Measurement and estimation of i_{cat} with i_{cat}-based observer. i_u sensor fault

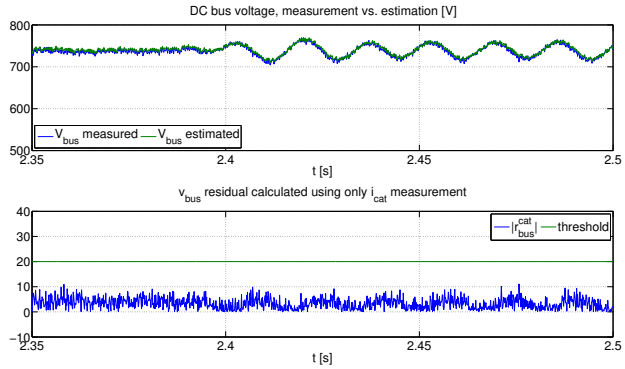

Fig. 15. Measurement and estimation of v_{bus} with i_{cat}-based observer. i_u sensor fault

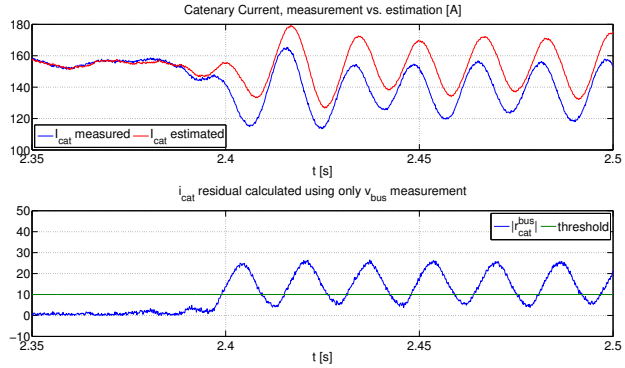

Fig. 16. Measurement and estimation of i_{cat} with v_{bus}-based observer. i_u sensor fault

V. Conclusions

This paper has presented the development of a state observer-based sensor FDI strategy for electric drives. Comparing to other strategies that model the electric motor, the approach described in this article uses the model of the input filter to estimate catenary current and DC-Link voltage. Hence, a greater level of immunity to parameter variation is achieved since capacitor and inductance parameters tend to change less than motor parameters. It has been shown that the strategy can effectively detect and isolate faults in the catenary current sensor and the DC-Link voltage sensor. In addition, the strategy has the ability to effectively isolate other sensor faults (v_{cat}, i_u, i_v, i_{crw}). Moreover, thanks to the bank of observers,

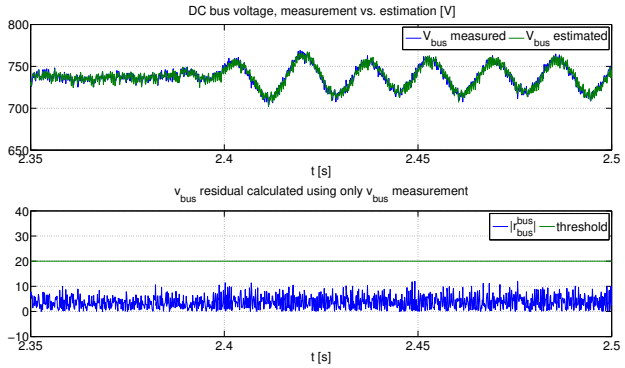

Fig. 17. Measurement and estimation of v_{bus} with v_{bus}-based observer. i_u sensor fault

there is always one estimation available for reconfiguration.

REFERENCES

[1] S. Bennett, R. Patton, S. Daley, and D. Newon, "Torque and flux estimation for a rail traction system in the presence of intermittent sensor faults," *UKACC International Conference on Control*, vol. 1, no. 427, pp. 72–77, 1996.

[2] T. A. Najafabadi, F. R. Salmasi, and P. Jabehdar-maralani, "Detection and Isolation of Speed- , DC-Link Voltage- , and Current-Sensor Faults Based on an Adaptive Observer in Induction-Motor Drives," *IEEE Transactions on Industrial Electronics*, vol. 58, no. 5, pp. 1662–1672, 2011.

[3] I. Jlassi, J. O. Estima, S. Khojet El Khil, N. M. Bellaaj, and A. J. M. Cardoso, "A Robust Observer-Based Method for IGBTs and Current Sensors Fault Diagnosis in Voltage-Source Inverters of PMSM Drives," *IEEE Transactions on Industry Applications*, vol. pp, no. 99, pp. 1–1, 2016.

[4] H. Berriri, M. W. Naouar, and I. Slama-Belkhodja, "Easy and fast sensor fault detection and isolation algorithm for electrical drives," *IEEE Transactions on Power Electronics*, vol. 27, no. 2, pp. 490–499, 2012.

[5] B. H. Lee, N. J. Jeon, and H. C. Lee, "Current Sensor Fault Detection and Isolation of the driving motor for an In-wheel Motor Drive Vehicle," in *International Conference on Control, Automation and Systems*, 2011, pp. 486–491.

[6] S. Fan and J. Zou, "Sensor Fault detection and fault tolerant control of induction motor drivers for electric vehicles," in *7th International Power Electronics and Motion Control Conference*, 2012, pp. 1306–1309.

[7] T. Achour and M. Pietrzak-David, "Service continuity of an IM distributed railway traction with a speed sensor fault," in *European Conference on Power Electronics and Applications (EPE)*, Achour2011, 2011, pp. 1–8.

[8] J. Guzinski, M. Diguet, Z. Krzeminski, A. Lewicki, and H. Abu-rub, "Application of Speed and Load Torque Observers in High-Speed Train Drive for Diagnostic Purposes," *IEEE Transactions on Industrial Electronics*, vol. 56, no. 1, pp. 248–256, 2009.

[9] Z. Peroutka, K. Zeman, F. Krus, and F. Kosta, "New Generation of Trams with Gearless Wheel PMSM Drives: From Simple Diagnostics to Sensorless Control," in *14th International Power Electronics and Motion Control Conference (EPE-PEMC)*, 2010.

[10] N. M. A. Freire, J. O. Estima, and A. J. M. Cardoso, "A new approach for current sensor fault diagnosis in PMSG drives for wind energy conversion systems," *IEEE Transactions on Industry Applications*, vol. 50, no. 2, pp. 1206–1214, 2014.

[11] D. Diallo, S. Member, and S. Diao, "Current Sensor Fault Estimation in the (d , q) rotating synchronous frame," in *IEEE Industrial Electronics Society Conference (IECON)*, 2016, pp. 0–5.

[12] D.-W. C. D.-W. Chung and S.-K. S. S.-K. Sul, "Analysis and compensation of current measurement error in vector-controlled AC motor drives," *IEEE Transactions on Industry Applications*, vol. 34, no. 2, 1998.

[13] H.-s. Jung, J.-m. Kim, C. Kim, and C. Choi, "Diminution of Current Measurement Error For Vector Controlled AC Motor Drives," in *IEEE Transactions on Industry Applications*, 2005, pp. 551–557.

[14] A. B. Youssef, S. K. El Khil, and I. Slama-Belkhodja, "State Observer-Based Sensor Fault Detection and Isolation, and Fault Tolerant Control of a Single-Phase PWM Rectifier for Electric Railway Traction," *IEEE Transactions on Power Electronics*, vol. 28, no. 12, pp. 5842–5853, 2013.

[15] A. Ben Youssef, S. K. E. Khil, and I. Slama-Belkhodja, "DC Bus Sensor Fault Tolerant Control of Single Phase PWM Rectifer for Electrical Traction," in *8th Internationl Multi-Conference on Systems, Signals & Devices*, 2011, pp. 1–6.

[16] Y. S. Jeong, S. K. Sul, S. E. Schulz, and N. R. Patel, "Fault detection and fault-tolerant control of interior permanent-magnet motor drive system for electric vehicle," *IEEE Transactions on Industry Applications*, vol. 41, no. 1, pp. 46–51, 2005.

[17] G. H. Foo, X. Zhang, and D. M. Vilathgamuwa, "A Sensor Fault Detection and Isolation Method in Interior Permanent-Magnet Synchronous Motor Drives Based on an Extended Kalman Filter," *IEEE Transactions on Industrial Electronics*, vol. 60, no. 8, pp. 3485–3495, 2013.

[18] S. M. Jung, J. S. Park, H. W. Kim, K. Y. Cho, and M. J. Youn, "An MRAS-based diagnosis of open-circuit fault in PWM voltage-source inverters for PM synchronous motor drive systems," *IEEE Transactions on Power Electronics*, vol. 28, no. 5, pp. 2514–2526, 2013.

[19] M. Fadali and A. Visioli, *Digital control engineering: analysis and design*. Academic press, 2012.

[20] G. Ellis, *Observers in control systems: a practical guide*. Academic press, 2002.

VI. BIOGRAPHIES

Jon del Olmo was born in Oiartzun, Spain in 1988. He received the B.S. and M.S. degrees in Electronics Engineering from the University of Mondragón, Mondragón, Spain, in 2009 and 2012, where he is currently working toward the PhD. degree in the Department of Electronics, Faculty of Engineering. His current research interests include electric drives, fault detection and diagnostics.

Fernando Garramiola was born in Eibar, Spain in 1975. He received the B.S. and M.S. degrees in Electrical Engineering from the University of Mondragón University, Mondragón, Spain, in 1997 and 1999, and the MPhil degree in Electrical Engineering from Heriot-Watt University, Edinburgh, UK, in 2001. Since 2010, he is with the Electronics and Informatics Department, Faculty of Engineering, University of Mondragón. His current research interests include electric drives, maintenance and model-based fault diagnosis.

Javier Poza was born in Bergara, Spain, in June 1975. He received the B.S. and M.S. degrees in Electrical Engineering from the University of Mondragón, Mondragón, Spain, in 1997 and 1999, and the Ph.D. degree in Electrical Engineering from the INP, Grenoble, France. Since 2003, he is with the Department of Electronics, Faculty of Engineering, University of Mondragón, where he is currently an Associate Professor. His current research interests include electrical machine design, modelling, and control. He has participated in various research projects in the fields of wind energy systems, lift drives, electric vehicles and railway traction.

Txomin Nieva was born in San Sebastian, Spain in 1972. He received a Computer Science Engineering degree in 1997 and a System Engineering degree in 1998 from the University of Mondragón, Spain, and a PhD in Computer Science from the EPFL, Switzerland, in 2001. Currently he is working as Technical Director of CAF Power Automation. His research areas are in power electronics in general and electrical traction systems in particular.

Gaizka Almandoz was born in Arantza, Spain, in March 1979. He received the B.S. and Ph.D. degrees in Electrical Engineering at the University of Mondragón, Mondragón, Spain, in 2003 and 2008, respectively. Since 2003, he is with the Department of Electronics, Faculty of Engineering, University of Mondragón, where he is currently an Associate Professor. His current research interests include electrical machine design, modelling, and control. He has participated in various research projects in the fields of wind energy systems, lift drives, and railway traction.

Leire Aldasoro was born in a town near San Sebastian, Spain in 1981. She received the Industrial Engineering degree in 2005 from the University of Navarra (Tecnun). After working on the first traction system developed by CAF in its research and development area, currently she is the responsible of the Power Electronics Product Development group in CAF Power Automation. Her research area is electrical traction systems in general, focused on systems control algorithms